

P. Clari · L. Fornara · B. Ricci · G. M. Zuppi

Methane-derived carbonates and chemosymbiotic communities of Piedmont (Miocene, northern Italy): An update

Received: 30 September 1993 / Revision received: 29 March 1994

Abstract Stable carbon isotope values of authigenic carbonate rocks in the Miocene terrigenous sediments of Piedmont indicate a methane-related origin. Some of these methane-derived carbonates (*Lucina* limestone) are characterized by the presence of abundant lucinid remains. Carbonate dissolution/precipitation and development of lucinid communities were related to bacterial methane oxidation, both aerobic and anaerobic. Anaerobic oxidation led to carbonate precipitation and production of sulfide, which sustained lucinid communities through chemosynthetic symbiotic bacteria. Aerobic oxidation of methane likely resulted in dissolution of carbonate skeletal grains. Several phases of carbonate precipitation, characterized by slightly different isotopic compositions, are recognizable in the limestones.

Introduction

Six years ago we described authigenic, methane-derived carbonates and stratigraphically restricted, large-bivalve communities in the terrigenous sediments of Miocene age in Piedmont (Clari et al. 1988). At that time we advanced the hypothesis of a close and widespread relationship between methane-derived carbonates and specialized bivalve communities. Our hypothesis was supported by the isotopic compositions of the carbonates (consistently depleted in ^{13}C) and by the few examples we knew at the time of modern cold-vent-related biotic communities and authigenic carbonates (Kulm et al. 1986; Ritger et al. 1987; Hovland et al. 1987). Fossil examples of such cold-vent communities were, at that time, almost unknown except for the Jurassic "pseudobioherms" of Beauvoisin (Gaillard et al. 1985).

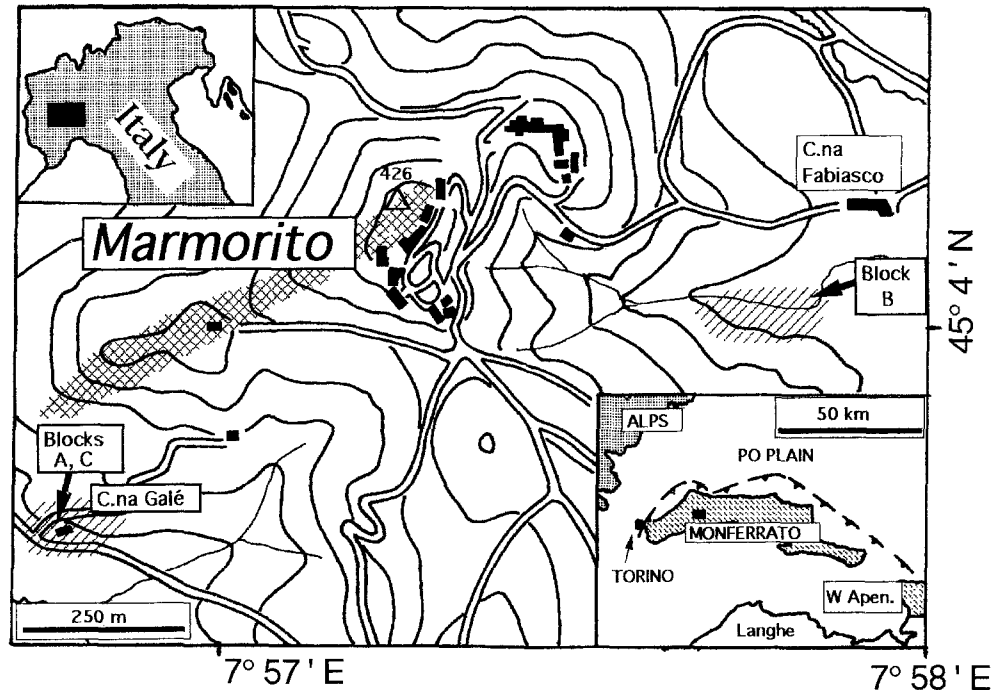
The purpose of this paper is to update our 1988 description in light of later publications (e.g., Goedert and Squires 1990; Beauchamp and Savard 1992; Campbell 1992) and the results of our ongoing field and laboratory work. In particular, this paper focuses on the petrographic textures and isotope geochemistry of some of the carbonate facies occurring in the Marmorito area (*Lucina* limestone, see later) and represents a further step toward better insights into the range of geological factors that led to the formation and preservation of these rocks.

Occurrence of carbonate facies

The unusual sedimentary carbonates, the subject of this study, occur in small outcrops near the village of Marmorito in the Monferrato hills, east of Torino (Fig. 1). Some aspects of the local geology are unsatisfactorily known because of the extensive Quaternary cover, absence of fossils in many facies, and strong syn- and postdepositional tectonic activity affecting this area during the entire Miocene (Piana and Polino, unpublished data). However, the Monferrato area, located behind the most recent frontal Apenninic thrusts, is presently interpreted as a strongly deformed episutural basin (or basins), which developed from Eocene to Miocene on a Late Cretaceous accretionary prism. The Oligo-Miocene sedimentary succession in the western sector of Monferrato, where carbonate facies are found, consists mostly of coarse- to fine-grained siliciclastic sediments deposited in a slope to inner shelf environment (Clari et al. 1988 and unpublished data). Uncommon diatomitic facies occur in the Marmorito area (Bonci et al. 1990). The siliciclastic-diatomitic succession is truncated at the top by a subaerial erosional surface due to the dramatic relative fall of the sea level during the Messinian salinity crisis. A shallowing-upward succession of silty clays and weakly cemented sandstones of Pliocene age rests unconformably on this erosional surface.

Around Marmorito, two different types of carbonates occur. One is a cream- to light-brown-colored marly lime-

Fig. 1 Location of the outcrops of methane-derived limestones. Cross-hatching: area of outcrop of carbonate-enriched terrigenous sediments (Marmorito limestones). Oblique ruling: areas where scattered blocks of *Lucina* limestone were found near the farms Cascina Galé and Cascina Fabiasco. Lower right inset: Location of the Marmorito area (black rectangle) in central Piedmont



stone, packed with bivalve (*Lucina*) remains (*Lucina* limestone; Clari et al. 1988). The other is a light to dark grey, calcite- and dolomite-cemented mudstone and sandstone crosscut by calcitic veins. The strongly cemented mudstone is generally extremely hard and brittle and resembles micritic limestones or dolostones. These rocks, which appear to be barren of fossils, were labeled as Marmorito limestone (Clari et al. 1988).

The *Lucina* limestone, because of its very unusual fossil assemblages, has attracted the attention of geologists and paleontologists since the beginning of 19th century (Sacco 1901). However, the fossil assemblage and the geologic framework of the Marmorito carbonate sediments were never the subject of detailed studies, as were analogous facies in the northern Apennines (e.g., Moroni 1966; Ricci Lucchi and Veggiani 1967).

Macroscopic fossil content of the *Lucina* limestone consists almost exclusively of articulated, large, thick-shelled clams of its namesake. A precise taxonomic identification of these bivalves is uncertain, as most specimens are preserved as molds, which are commonly deformed. More than one species may be represented; the most abundant species may be referred to the genus *Anodontia* (*A. dicomani*, L. Motta personal communication 1992).

Field research failed to document any lateral transition between the *Lucina* limestone and the Marmorito limestone. The hard "microcrystalline" facies of the Marmorito limestone and dolostone are found as localized diagenetic transformation of the "normal" siliciclastic facies of the Miocene succession, through the addition of a significant amount of carbonate cement. Locally it is possible to laterally follow the transition from hard, carbonate-cemented mudstones and sandstones to softer, compacted and slightly cemented siliciclastic facies.

The *Lucina* limestone, in contrast, is found only as meter-scale blocks, smaller clasts, and isolated lucinid internal molds scattered in the fields or heaped by farmers along the field edges. Two large concentrations of blocks and clasts were sampled near the small farms called Cascina Galé and Cascina Fabiasco (Fig. 1). At the first locality, the blocks and some boulders (up to 4 m) seem to be part of a debris-flow accumulated in a local depression of the Messinian erosional surface. At the second site, the blocks appear to have been involved in a Recent landslide and certainly suffered also from intensive reworking due to farming activities. In both sites hence the original sedimentary framework of these carbonate masses is lost.

Analytical techniques

More than 100 thin sections of the carbonates were prepared for microscopic examination. Selected sections were polished and observed under a scanning electron microscope (SEM) and cathodoluminescence. Few electron microprobe (EDX) analyses have been performed in order to identify carbonate phases and pyrite. The content of carbonate relative to fine- and coarse-grained terrigenous material was determined for five representative samples.

Drilled samples for stable carbon and oxygen isotope analyses were treated with orthophosphoric acid in accordance with the standard procedure described by McCrea (1950). The $^{13}\text{C}/^{12}\text{C}$ and $^{18}\text{O}/^{16}\text{O}$ ratios of the evolved CO_2 were measured on a Varian-Mat 250 mass spectrometer according to established techniques. The results are reported in delta (δ) notation in per mil (‰) relative to the PDB standard.

Results

Petrography

Petrographic analysis of the *Lucina* limestone documents that it derives from precipitation of authigenic carbonate in the pores of an original fine-grained siliciclastic sediment.

Three of the sampled and studied blocks of *Lucina* limestone will be described here as examples of successive stages of (dia)genetic evolution of this limestone.

Block A

This quite large (max dimension > 3 m) block was sampled in the Cascina Galé debris flow. It consists of yellowish marly micritic limestone with abundant lucinid “composite molds.” The molds show articulated valves, are slightly deformed by compaction, and average 12 cm in length and may reach 18 cm (Fig. 2A). The original shell material has been completely dissolved and the resulting voids closed under pressure of overburden superimposing the external and internal molds.

The “micritic” groundmass, surrounding and infilling

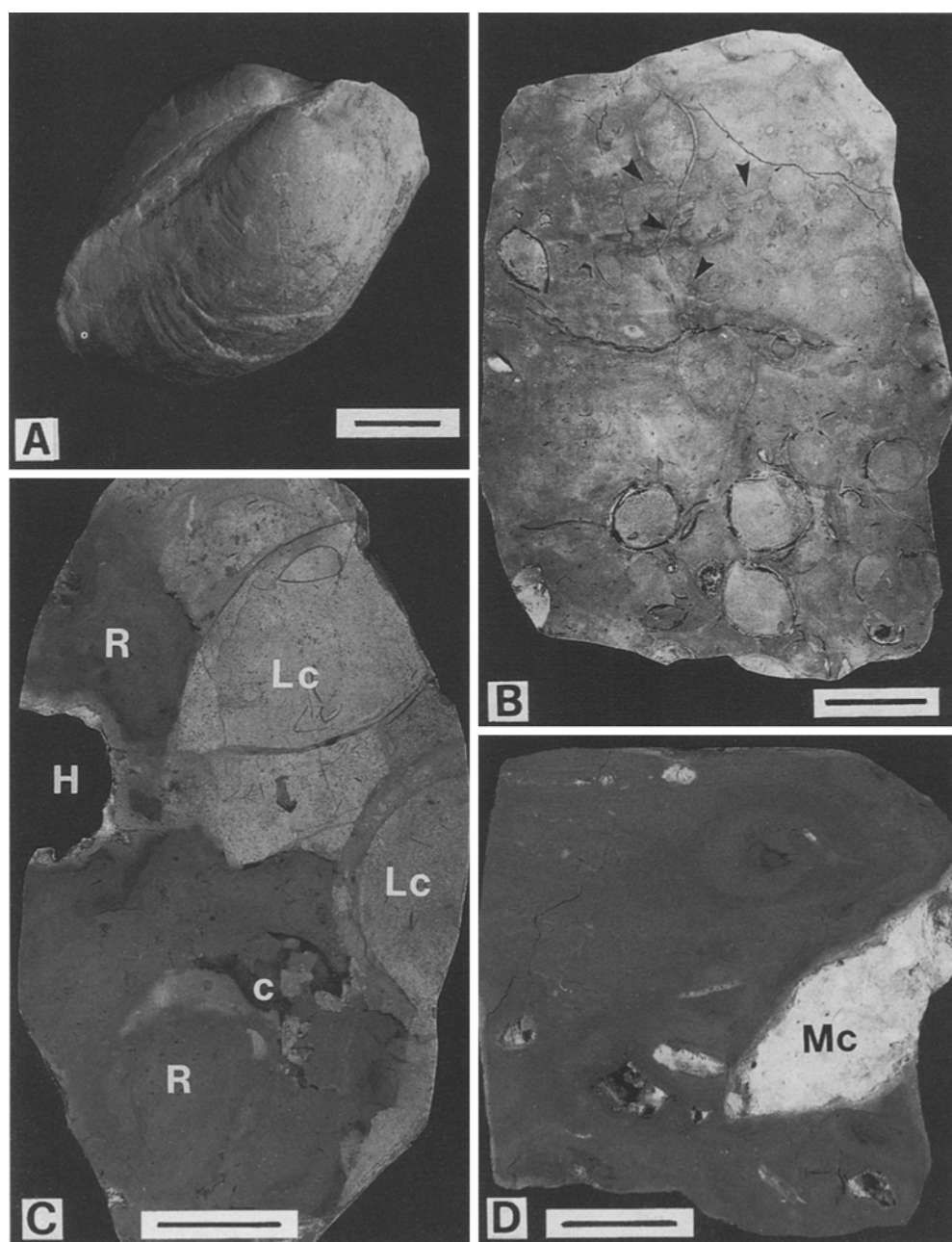


Fig. 2 A: Lucinid composite mold extracted from block A. Scale bar = 3 cm. B: Sawed surface of block B. Several lucinids are present. Original shells have been dissolved and the resulting voids were partially or completely filled by internal sediment. Different generations of burrows are also present. A network of sediment-filled burrows and/or fractures is recognizable (arrows). Scale bar = 20 cm. C: Sawed surface of block C. The recrystallized groundmass (R) and the “clasts” of *Lucina* limestone (Lc) are clearly recognizable. Calcite spar-filled cavities (c) are present. The irregular reentrant (H) is part of a cavity previously filled by white, incoherent microcrystalline calcite. Scale bar = 3 cm. D: Sawed surface of block C. This part of the block consists mainly of brown-gray recrystallized calcite with cavities filled by white, incoherent microcrystalline calcite (Mc). Two empty cavities are also present. Scale bar = 3 cm

the lucinid molds appears homogeneous and bioturbated. Faint dissolution seams and reddish stains are locally present.

In thin sections, the rock appears as a homogeneous, calcite-cemented, siliciclastic mudstone with sparse sand and silt-sized quartz and mica grains. Rusty and reddish colored grains and stains are widespread and likely resulted from the oxidation of pyrite framboids and grains. Microspar-filled voids suggest the presence of an original biogenic fraction consisting of planktonic and benthic foraminifer tests that were probably dissolved in an early diagenetic phase. The pore-filling calcite cement consists of micrometer-sized crystals.

Block B

This block, found at the edge of a field near Cascina Fabiasco, is a representative of the most common facies of the *Lucina* limestone. It was recovered complete (70 × 50 × 40 cm) and sawed into four thick slices for a closer inspection of its complex sedimentological features (Fig. 2B).

It consists of a yellowish “micritic” groundmass with isoriented, articulated lucinids remains. Original shells have been completely dissolved as in block A, but the resulting cavities are partially or completely filled by yellowish grey carbonate sediments and cements. The micritic groundmass is crosscut by an intertwined network of subvertical fissures and/or burrows that link together the cavities left by the dissolution of the shells. This network of cavities appears completely plugged by the same sediments that fill the voids left by shell dissolution.

The microfacies of the groundmass is similar to that of block A but for the presence of a substantial biogenic fraction, consisting mainly of tests of planktonic foraminifers (Fig. 3). Other common components are: benthic foraminifers, bivalve shell fragments, echinoid spines, and serpulid tubes. Iron-oxides and hydroxides are abundant as isolated grains and as fillings of foraminifer tests. Abundant fecal pellets, ovoidal in shape and up to 3 mm in length with diameters of about 1 mm, fill some small (1- to 3-cm) burrows.

Two types of internal sediments are recognizable in the network of cavities (shell voids, burrows, fractures): a first generation of “detrital” intraclastic and bioclastic sand- and silt-sized sediments, which rests on the floors of cavities. It is polyphasic and different phases of deposition are separated by cement fringes, which, owing to their diminutive size (maximum few millimeters), could not be isolated for analysis. A second generation of internal sediments, consisting of a sort of crystalline silt, postdates the detrital type and seems restricted to larger cavities (Fig. 4A).

Block C

The third block, again found in the Cascina Galé debris flow, is smaller than the other two (maximum dimension

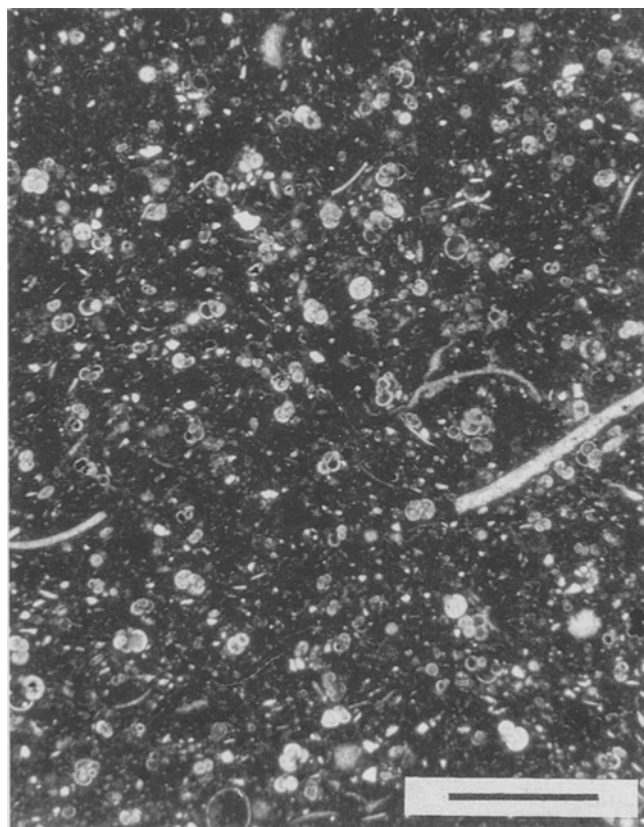
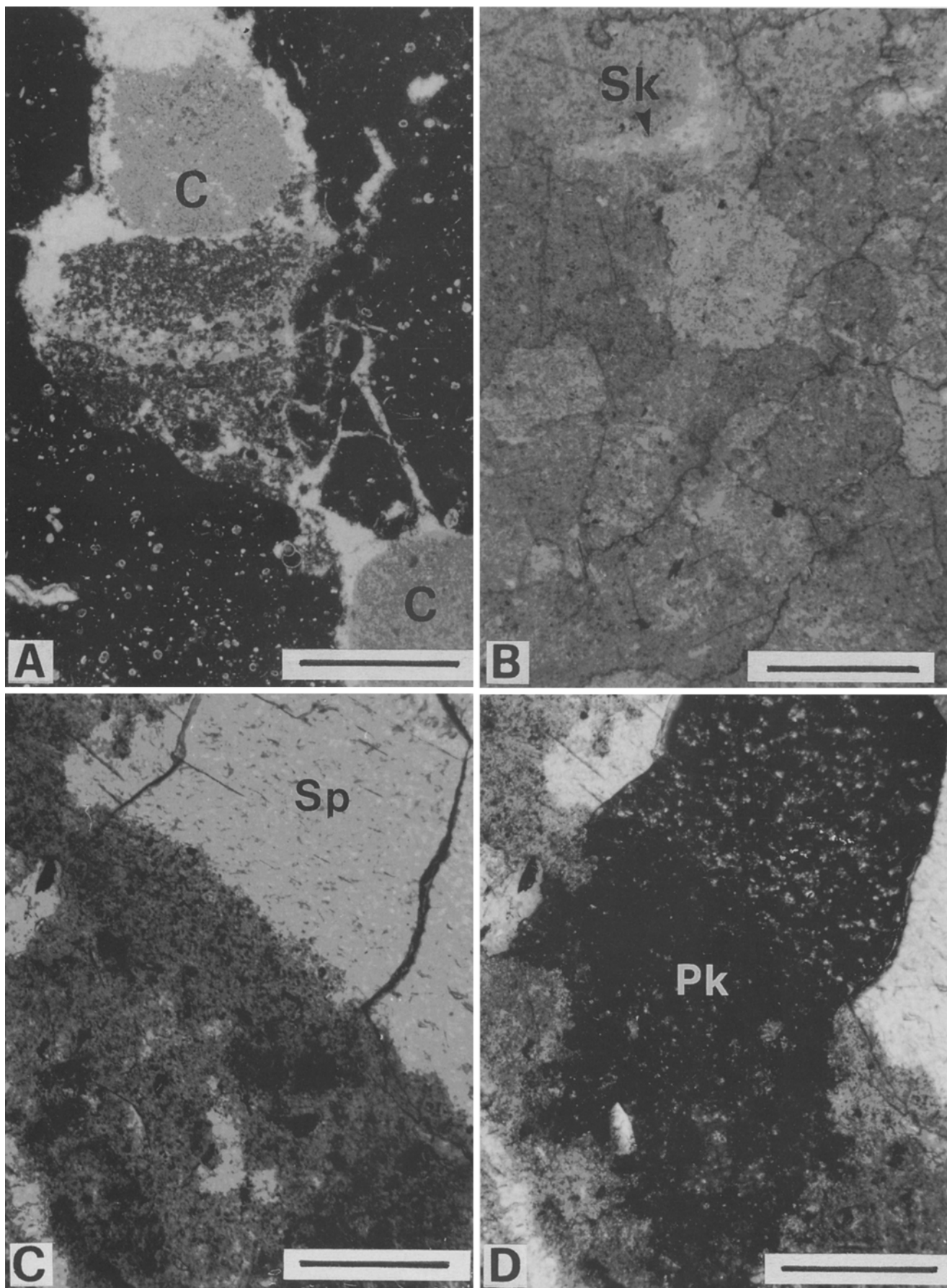


Fig. 3 Microfacies of the groundmass of block B. Plane light. Scale bar = 1 mm

35 cm) and shows peculiar macroscopic and microscopic features. It consists of a dark, brownish to gray, coarsely crystalline groundmass in which sparse, whole, or fragmentary lucinid molds and “clasts” of *Lucina* limestone are embedded (Fig. 2C). These molds and clasts consist of a whitish–yellowish marly limestone similar to the one forming the other two blocks, but it is locally friable and porous. The lucinid molds are generally incomplete, although they often retain part of the sediment-filled void left by the shell dissolution. The contact between the crystalline groundmass and the lucinid molds and clasts is locally sharp and clear-cut, whereas in other places it appears gradational.

Moreover, irregular, rounded to roughly tubular centimeter-sized cavities filled by a white, chalky micro-

Fig. 4 A: Polyphasic internal sediments filling cavities in block B. In the upper cavity two layers of intraclastic sediments are followed by a crystalline silt (C), which fills also the lower cavity. White areas are sparry calcite. Plane light. Scale bar = 1 mm. B: Recrystallization texture of the dark groundmass of block C. The irregular, sutured contacts among different poikilotopic crystals are easily recognizable. Ghosts of skeletal grains (Sk) are present. Plane light. Scale bar = 1 mm. C, D: Detail of void-filling cement in block B. C: plane light; D: crossed polars. The clear, void-filling sparry calcite (Sp) and the poikilotopic recrystallized calcite enclosing the terrigenous matrix (Pk) behave optically as a single crystal. Note the complex, sutured contacts of different optical domains in the recrystallized part and the simple, straight ones in the void-filling cement. Scale bar = 0.5 mm



crystalline calcite are present in the crystalline groundmass (Fig. 2D). When empty, these cavities display walls riddled by small ridges, tubular projections and even short, tubular bridges between opposite walls (Fig. 2C, D).

In thin sections, the groundmass of block C appears as a mosaic of tightly interlocking, anhedral, millimeter-sized calcitic crystals well recognizable especially at crossed polars. The boundaries among crystals are extremely complex and serrated (Fig. 4B). The single crystals engulf poikilotopically a siliciclastic clay-sized matrix with scattered larger quartz and mica grains. Ghost spar-filled molds of planktonic foraminifera and other bioclasts are locally recognizable (Fig. 4B). The clear calcite spar filling these molds is in optical continuity with the surrounding poikilotopic crystal. Larger cavities, deriving from dissolution of skeletal remains (lucinid shells, gastropods) or from other causes (bioturbation?) are filled by larger (up to centimeter-sized) calcitic crystals with straight crystalline boundaries. Void-filling crystals are in optical continuity with the crystals of the surrounding matrix and often engulf a first generation of internal sediments (Fig. 4C, D).

This texture clearly originated from a recrystallization of the facies of the *Lucina* limestones represented by block B. The new crystals grew poikilotopically in the siliciclastic fine-grained matrix, engulfing grains and infilling or substituting skeletal fragments. The serrated complex boundaries result from the competitive growth of poikilotopic crystals among the siliciclastic grains of the original sediment.

The microscopic texture of the yellowish marly limestone that forms the clasts and molds of lucinids is the same as that of other two blocks. Moldic porosity, resulting from skeletal grains dissolution, however, is only locally occluded by late spar.

The carbonate content of the groundmass of the three

blocks ranges from 85.2% for block A to 95.1% for the brown recrystallized matrix of block C. These values, which are well above the range of initial porosity values common in marine mudstones (i.e., 70–80%), result from the addition of a substantial quantity of diagenetic pore-filling cement to the skeletal carbonate present in the original siliciclastic sediment.

Stable isotopes

More than 30 analyses of carbon and oxygen isotopes have been performed on the limestones (Clari et al. 1988; Fornara unpublished data). The results of the most recent analyses, performed on the three above-described blocks are summarized in Table 1 and Figs. 5 and 6. Nearly all the carbonate phases analyzed (both micritic matrix and

Table 1 Stable isotope values of samples analyzed in permil relative to PDB standard

| Samples | $\delta^{13}\text{C}$ | $\delta^{18}\text{O}$ |
|--|-----------------------|-----------------------|
| Block A | | |
| A1: Micritic groundmass | -30.4 | +4.9 |
| A2: Micritic groundmass | -30.4 | +4.9 |
| A3: Lucinid mold | -30.6 | +4.9 |
| Block B | | |
| B1: Micritic groundmass | -27.6 | +0.4 |
| B2: Lucinid mold | -25.2 | +0.1 |
| B3: Lucinid mold | -25.6 | +0.5 |
| B4: Sediment filling shell void | -26.7 | +0.9 |
| B5: Sediment filling shell void | -12.2 | +0.5 |
| B6: Sediment filling the network of "fractures" | -35.5 | +0.8 |
| B7: Sediment filling the network of "fractures" | -32.7 | +0.8 |
| B8: Sediment filling the network of "fractures" | -30.7 | +0.7 |
| Block C | | |
| C1: Lucinid mold | -27.9 | +4.4 |
| C2: Recrystallized matrix | -17.8 | +2.6 |
| C3: Recrystallized matrix | -17.6 | +2.7 |
| C4: Void-filling incoherent microcrystalline calcite | -0.1 | +4.8 |

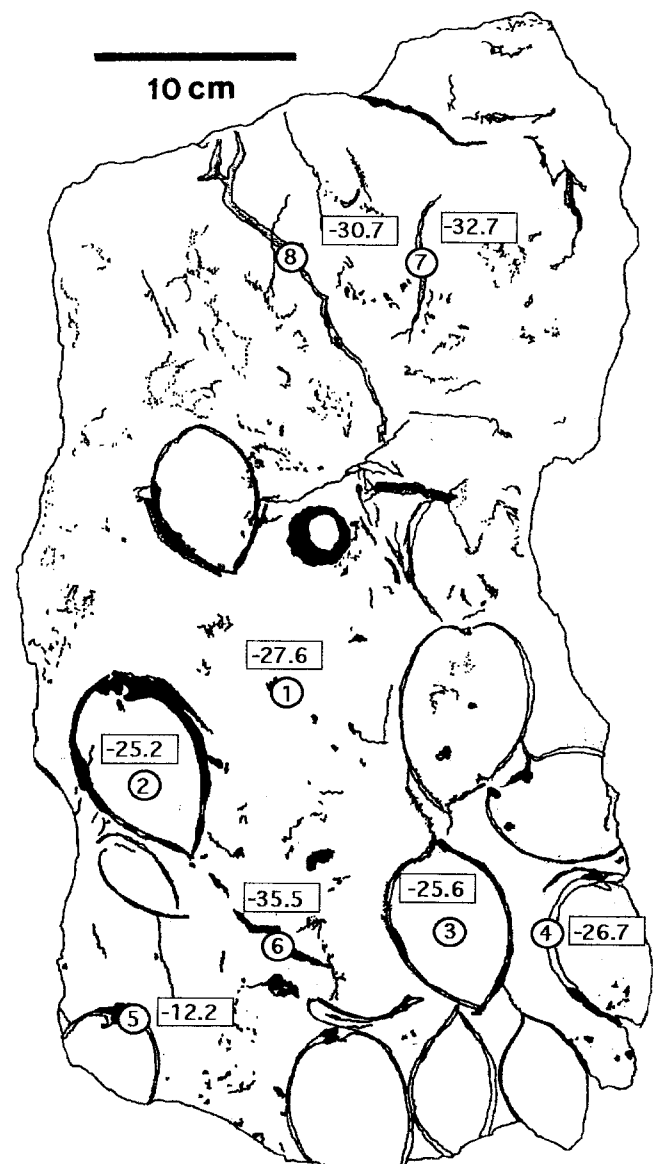


Fig. 5 Sketch of a sawed surface of the block B with $\delta^{13}\text{C}$ values of samples B1–B8. See also Fig. 6 and Table 1

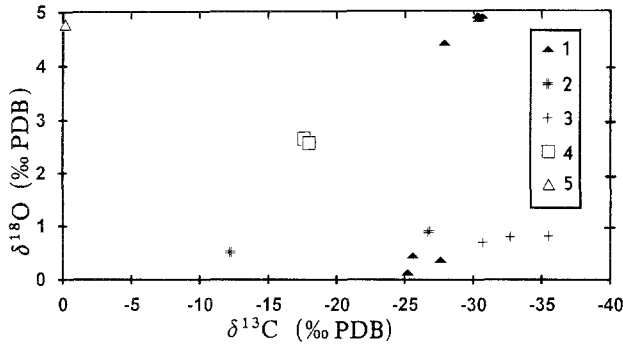


Fig. 6 Plot of the isotopic values of the analyzed samples. 1. Micritic groundmass (blocks A, B, C) 2. Sediment filling shell-voids (block B) 3. Fracture-filling sediment (block B) 4. Recrystallized matrix of block C 5. White microcrystalline calcite filling irregular voids (block C)

internal sediments and/or cements) yielded strongly negative $\delta^{13}\text{C}$ values ranging from -25‰ to -35‰ . Less negative values characterize the composite sedimentary infilling of some shell voids in block B (-12‰) and the recrystallized matrix of block C (-17‰). The white, microcrystalline calcite filling the irregular cavities in block C, however, yielded a markedly different $\delta^{13}\text{C}$ of -0.1‰ .

The strongly negative $\delta^{13}\text{C}$ signature characterizing most carbonate phases of the *Lucina* limestone is universally recognized as the best evidence of a methane-related origin (e.g., Ritger et al. 1987; Hovland et al. 1987; Campbell 1992).

The extremely depleted carbon isotope composition of methane ($\delta^{13}\text{C}$ ranging from -35‰ to -50‰ for thermogenic methane and less than -60‰ for biogenic one; Claypool and Kaplan 1974 in Beauchamp and Savard 1992) leads to this unusually negative isotopic signature of the derived carbonate phases. The actual range of $\delta^{13}\text{C}$ of the resulting carbonates depends on the relative contributions of carbon from methane and from other sources, i.e., the inorganic bicarbonate pool and marine organic carbon (Paull et al. 1989, 1992). Control analyses performed on tests of planktonic and benthic foraminifers isolated from coheval siliciclastic sediments resulted in "normal" $\delta^{13}\text{C}$ ranging from $+1.2\text{‰}$ to -2‰ . The $\delta^{13}\text{C}$ values of *Lucina* limestones suggest, therefore, a variable mixing of CO_2 coming from different sources. The different contributions to mixing of carbon reservoirs change slightly from block to block, suggesting an areally variable flux of methane-rich fluids. On the other hand, the larger variations of $\delta^{13}\text{C}$ from matrix to veins and from vein to vein in a single block suggest that the rate of methane-rich fluid venting fluctuated in time, as happens in present-day venting sites. The $\delta^{13}\text{C}$ values obtained for the recrystallized dark matrix of block C (-17‰) and for the white incoherent cavity-filling, microcrystalline calcite (-0.1‰) would deserve elaborate discussion, if confirmed by a new set of analyses now under way. For the moment, the more likely explanation is that the strongly ^{13}C -depleted carbon isotopic composition of the *Lucina* limestone was changed

during late diagenetic (re)crystallization phases after the demise of fluid venting.

Oxygen isotopic measurements yielded $\delta^{18}\text{O}$ values of $0.1\text{--}4.9\text{‰}$ relative to the PDB standard. The relatively narrow range of the positive $\delta^{18}\text{O}$ values implies that all carbonates precipitated and recrystallized from waters of similar, relatively low, temperatures and seems to rule out the possibility of a late diagenetic recrystallization of the matrix of block C in meteoric waters.

Genesis and diagenesis of *Lucina* limestone

The development of dense lucinid communities and the precipitation around them of ^{13}C -depleted carbonates are here interpreted as the biological and sedimentary by-products of sea-floor venting of methane-charged fluids.

No data on the nutritional strategies of present-day, vent-related lucinid clams are known. However, many living species of lucinaceans host in the gills symbiotic sulfide-oxidizing bacteria (Turner 1985; Reid and Brand 1986; Cary et al. 1989), whereas no living species is known to possess the methane-oxidizing symbionts that have been found in other vent-related organisms (Childress et al. 1986; Brooks et al. 1987). In this context, it is reasonable to infer that the *Lucina* limestone communities were sustained, at least in part, by the sulfide generated in the pore waters of the sulfate-reducing zone through anaerobic bacterial oxidation of a diffuse flux of methane. The bacterial oxidation of methane can occur both aerobically and anaerobically in the pore waters of the oxic and sulfate-reducing zone respectively. When an upward flux of methane enters the sulfate-reducing zone, methane-oxidizing bacteria provide the energy source for sulfate reducers, and the coupled process results in the production of bicarbonate (HCO_3^-) and hydrogen sulfide (H_2S^-) (Hovland et al. 1987; Jørgensen 1989; Ritger et al. 1987; Beauchamp and Savard 1992). At the Marmorito paleovent, the supply of sulfide was not exhausted by authigenic pyrite formation and could sustain symbiotic and free-living chemotrophic bacteria; it eventually diffused upward through the sediments, reaching the oxic zone.

A reconstruction of the successive genetic and diagenetic stages of the *Lucina* limestone may be so delineated:

1. An area of diffuse methane-rich fluid venting was colonized by a dense, specialized community dominated by large infaunal lucinid clams. These were sustained by a chemosynthetic food chain supported by sulfide. As observed for living species (Turner 1985), the clams lived buried into the sediment close to the interface between oxic and anaerobic (sulfate-reducing) zones. They fed tapping the pore waters of the sulfate-reducing zone rich in sulfide produced by sulfate-reducing bacteria and bacterial anaerobic oxidation of methane. The diffuse upward-migrating flux of methane caused, moreover, carbonate dissolution in the oxic zone contemporaneous with carbonate precipitation in the sulfate-reducing zone, through aerobic and

anaerobic bacterial activity, respectively. In the oxic pore water of the sediments surrounding living clams, in fact, aerobic oxidation of migrating methane caused a decrease in pH (Matsumoto 1990) and a consequent dissolution of skeletal carbonate. This carbonate dissolution could be locally enhanced by oxidation of sulfide diffusing upward from the sulfate-reduction zone. In present-day vent environments the dissolution of bivalve shells is severe and affects both infaunal and epifaunal forms. Traces of dissolution are present also on living specimens (Callender and Powell 1992). In the Marmorito paleovent, the dissolution of lucinid shells was completed near the sediment/water interface as evidenced by the sedimentary fills of the shell cavities.

2. With continuing sedimentation the oxic/anoxic interface slowly migrated upward and the sediments enclosing dead and partially or completely leached lucinid shells passed through the sulfate-reducing zone. Here the precipitation of the finely crystalline, ^{13}C -depleted, authigenic carbonates forming the *Lucina* limestone groundmass took place in the pores of the siliciclastic sediment. In the pore waters of the sulfate-reducing zone, in fact, the alkalinity was drastically increased by HCO_3^- produced by anaerobic methane oxidation.

The methane-related phase in the history of the *Lucina* limestone of block A probably ended here. Authigenic carbonate precipitation in the sulfate-reducing zone was not sufficient to prevent compaction of the sediments during burial, as indicated by deformation of lucinids composite molds.

3. A slightly different and longer history is registered in block B. In this case a more substantial precipitation of authigenic carbonate cement not only inhibited burial compaction but reduced the pore space blocking diffuse fluid flow. Methane-charged fluids were then channelized through a network of cavities consisting of shell-dissolution voids, burrows, and fractures. Sediment infilling and carbonate cement precipitation progressively reduced and eventually plugged this network of cavities also. Internal sediments and cements still show an overall negative $\delta^{13}\text{C}$ but single values are more variable due to the existence of different microenvironments characterized by a different percentage of available methane-derived carbon.

4. A later recrystallization phase, registered in block C, deeply changed locally carbonate textures and averaged the original isotopic signature. The diagenetic environment and the moment in which this recrystallization took place are still unclear.

Conclusions

1. Carbonate-rich sediments outcropping at Marmorito result from authigenic, methane-related precipitation of carbonate cements within unconsolidated siliciclastic sediments.

2. The *Lucina* limestone represents a good example of

the geological results of cold-vent-related processes, both organic and inorganic. These unusually dense communities of large bivalves enclosed in an isotopically light carbonate groundmass are evidence of a long and complex history of methane-rich fluid venting through the sea floor.

3. The diffusion of methane-rich fluids through the sea floor supported dense ecosystems dominated by infaunal, soft-bottom-dwelling bivalves fed by symbiotic, chemoautotrophic, sulfide-oxidizing bacteria. With continuing sedimentation, the dead bivalves and the enclosing sediments passed through the oxic/anoxic interface and entered the sulfate-reducing zone. Here, anaerobic bacterial degradation of CH_4 induced intense carbonate precipitation into sediment pore spaces. The strongly negative carbon isotopic signature of the authigenic carbonate, which forms the micritic groundmass enclosing the bivalve remains, results from the incorporation of methane-derived CO_2 .

4. The precipitation of pore-filling carbonate reduced available pore space for fluid movement and hindered diffuse fluid venting. Methane-charged fluids then enlarged and/or opened new paths through voids left by the early dissolution of bivalve shells and by the activity of unknown burrowers. These new pathways were progressively reduced and eventually plugged by several generations of internal sediments and cements, which still incorporate a variable percentage of isotopically light carbon generated by bacterial methane oxidation.

5. In some cases a later recrystallization phase deeply changed carbonate textures and altered the original isotopic signature.

Acknowledgments The authors wish to thank Anna Conti and Luca Martire for their invaluable help in the isotope analyses and carbonate content determination respectively. Luca Martire also helped with photographs and critical reading of the manuscript. Special thank to Claudia Terzi, who put at our disposal her large bibliography on cold vents.

References

- Beauchamp B and Savard M (1992) Cretaceous chemosynthetic carbonate mounds in the Canadian Arctic. *Palaios* 7:434–450
- Bonci C, Clari P, Ferrero E, Ghibaudo G, Pirini C, Ricci B, Valleri G, and Violanti D (1990) The Diatomites of Marmorito (western Monferrato, northern Italy). *Memorie di Scienze Geologiche* 42: 189–225
- Brooks JM, Kennicutt MC II, Fisher CR, Macko SA, Cole K, Childress JJ, Bidigare RR, and Vetter RD (1987) Deep-sea hydrocarbon seep communities: Evidence for energy and nutritional carbon sources. *Science* 238:1138–1142
- Callender WR and Powell EN (1992) Taphonomic signature of petroleum seep assemblages on the Louisiana upper continental slope: Recognition of autochthonous shell beds in the fossil record. *Palaios* 7:388–408
- Campbell KA (1992) Recognition of ancient cold seep biota from the northeast Pacific convergent margin. *Palaios* 7:422–433
- Cary SC, Vetter RD, and Felbeck H (1989) Habitat characterization and nutritional strategies of the endosymbiont-bearing bivalve *Lucinoma aequizonata*. *Marine Ecology Progress Series* 55:31–45
- Childress JJ, Fisher CR, Brooks JM, Kennicutt MC II, Bidigare R, and Anderson AE (1986) A methanotrophic marine molluscan

- (Bivalvia, Mytilidae) symbiosis: Mussel fueled by gas. *Science* 233:1306–1308
- Clari P, Gagliardi C, Governa ME, Ricci B, and Zuppi GM (1988) I Calcari di Marmorito: Una testimonianza di processi diagenetici in presenza di metano. *Bollettino Museo Regionale Scienze Naturali Torino*, 6:197–216
- Gaillard C, Bourseau JP, Boudeulle M, Pailleret P, Rio M, and Roux M (1985) Les pseudo-biohermes de Beauvoisin (Drome): Un site hydrothermal sur la marge tethysienne à l'Oxfordien? *Bulletin de la Société Géologique de France* 1:69–78
- Goedert JL and Squires RL (1990) Eocene deep-sea communities in localized limestones formed by subduction-related methane seeps, southwestern Washington. *Geology* 18:1182–1185
- Hovland M, Talbot M, Qvale H, Olausen S, and Aasberg L (1987) Methane-related carbonate cements in pockmarks of the North Sea. *Journal of Sedimentary Petrology* 57:881–892
- Jørgensen NO (1989) Holocene methane-derived, dolomite-cemented sandstone pillars from the Kattegat, Denmark. *Marine Geology* 88:71–81
- Kulm LD, Suess E, Moore JC, Carson B, Lewis BT, Ritger SD, Kadko DC, Thornburg TM, Embley RW, Rugh WD, Massoth GJ, Langseth MG, Cochrane GR, and Scamman RL (1986) Oregon subduction zone: Venting, fauna and carbonates. *Science* 231:561–566
- Matsumoto R (1990) Vuggy carbonate crust formed by hydrocarbon seepage on the continental shelf of Baffin Island, northeast Canada. *Geochemical Journal* 24:143–158
- McCrea JM (1950) On the isotope chemistry of carbonates and a paleotemperature scale. *Journal of Chemical Physics* 18:849–857
- Moroni AM (1966) Malacofauna del "calcare a Lucine" di S. Sofia-Forlì. *Paleontographia Italica* 60:69–87
- Pauli CK, Martens CS, Chanton JP, Neumann AC, Coston JA, Jull AJT, and Toolin LT (1989) Old carbon in living organisms and young CaCO₃ cements from abyssal brine seeps. *Nature* 342:166–168
- Pauli CK, Chanton JP, Neumann AC, Coston JA, Martens CS, and Showers W (1992) Indicators of methane-derived carbonates and chemosynthetic organic carbon deposits: Examples from the Florida Escarpment. *Palaios* 7:361–375
- Reid RGB and Brand DG (1986) Sulfide-oxidizing symbiosis in Lucinaceans: Implications for bivalve evolution. *The Veliger* 29:3–24
- Ricci Lucchi F and Veggiani A (1967) I calcari a *Lucina* della Formazione Marnoso-arenacea romagnola. Nota preliminare. *Giornale di Geologia* 34:159–172
- Ritger S, Carson B, and Suess E (1987) Methane-derived authigenic carbonates formed by subduction-induced pore-water expulsion along the Oregon/Washington margin. *Bulletin of the Geological Society of America* 98:147–156
- Sacco F (1901) Sul valore stratigrafico delle grandi Lucine dell'Appennino. *Bollettino della Società Geologica Italiana* 20:563–574
- Turner RD (1985) Notes on mollusks of deep-sea vents and reducing sediments. *American Malacological Bulletin Special Edition* 1:23–34